



Yoani Herrera, Aerodynamics Engineer  
 Altair Engineering  
 Troy, MI 48083

**To:** John Nagle Co.  
 306 Northern Avenue  
 Boston, MA 02210

**From:** Patrick Eyo, Jake Horcher, Mateo Sanchez, Jonah Shifrin; Testing Engineers.

**Subject:** Repurposing Farmland tanker trucks for transporting seafood

**Date:** November 27, 2020

**Distr:** Robert Nagle, Vice President Operations

## FOREWORD

Your company has reached out to us to help redesign trucks to improve fuel efficiency by reducing drag forces when traveling at highway speeds. This will require an analysis of the aerodynamic capabilities of each model to evaluate the optimal shape of cargo containers. Through the use of a wind tunnel, you requested that we determine the characteristics of the four containers on the 1:55 scale model trucks. The requirements are to achieve: calibration curves of the load cell and the manometer in your wind tunnel; plots of measured drag and lift forces as a function of calibrated air flow velocity for four model conditions; plots of drag and lift coefficients as a function of Reynolds number; the determination of one model container design that results in the minimal average drag coefficient within the measurement range of Reynolds number; and the drag and lift forces acting on a full-scale truck/container system at a moving speed of 65 miles/hr for the truck bearing the cargo container with the smallest drag. This report serves to document our methods, results with uncertainties, and recommendations for your purposes.

## SUMMARY

After conducting wind tunnel experiments at 1:55 scale on four truck/trailer combinations, varying the trailer geometry, we recommend the use of a trailer with a flat chamfer on the front top corner in order to minimize the drag coefficient. The testing of the provided model front angled trailer resulted in a drag coefficient of  $0.5 \pm 0.43$  and a lift coefficient of  $0.03 \pm 0.09$ . The full scale truck drag and lift force estimates were  $1700 \pm 1.4 \times 10^3$  N and  $330 \pm 8.8 \times 10^2$  N, respectively, assuming a truck velocity of 65 mph and still air. The scaled force estimation of each provided trailer geometry is depicted in Table 1 below.

**Table 1.** This table shows the estimated Reynolds numbers, drag coefficients and forces, and lift coefficients and forces for the full scale truck based on the data collected on the 1:55 scale models provided.

Trailer Shape	Avg. Drag Coefficient	Drag Force [N]	Avg. Lift Coefficient	Lift Force [N]	Estimated Reynolds Number
Box	$0.68 \pm 0.42$	$2300.8 \pm 1.4 \times 10^3$	$0.08 \pm 0.15$	$286.5 \pm 5.2 \times 10^2$	$1.4 \times 10^7 \pm 5.2 \times 10^5$
Angle Front	$0.50 \pm 0.43$	$1695.0 \pm 1.5 \times 10^3$	$0.03 \pm 0.09$	$122.6 \pm 3.3 \times 10^2$	$1.4 \times 10^7 \pm 5.2 \times 10^5$
Angle Back	$0.62 \pm 0.42$	$2103.6 \pm 1.4 \times 10^3$	$0.17 \pm 0.16$	$568.9 \pm 5.5 \times 10^2$	$1.4 \times 10^7 \pm 5.2 \times 10^5$
Curved Front	$0.54 \pm 0.42$	$1847.7 \pm 1.4 \times 10^3$	$0.08 \pm 0.15$	$267.3 \pm 5.1 \times 10^2$	$1.4 \times 10^7 \pm 5.2 \times 10^5$

We believe these quantities are not particularly accurate for three primary reasons: (1) the accuracy error of the load cell used was quite high, (2) the provided trailers do not appear to have a constant volume, and (3) the 1:55 and full scale model's Reynolds numbers are on opposite sides of the critical Reynolds number  $10^6$  [2] meaning they would not have the same drag coefficients as assumed above.

## METHODS

Analysis of our laboratory wind tunnel was performed to produce calibration curves for the drag load cell, lift load cell, and manometer used to measure wind speed. Wind tunnel tests were then performed on five different model trucks in order to produce plots of the lift and drag forces acting on the trucks versus wind speed, as well as to determine the drag and lift coefficients of the model trucks at each of the six different Reynolds numbers tested. Four of the model trucks had a trailer with a unique shape, and one truck had no trailer. A determination of the truck trailer shape with the lowest average drag coefficient was produced. Finally, the drag and lift forces on a full scale truck traveling at 65 miles per hour were calculated based on the model truck with the lowest drag coefficient.

## Equipment

The equipment used in the wind tunnel setup involved an *AeroLab* wind tunnel which has an accuracy of 0.50 mph and a resolution of 0.05 mph [1] with a precision percentage of 0.24%. The wind tunnel is equipped with a *Dwyer* 400 series inclined manometer with accuracy error of 2% and precision error of 0.005 inH<sub>2</sub>O for measurements below 1 inH<sub>2</sub>O and 0.05 inH<sub>2</sub>O for measurements above 1 inH<sub>2</sub>O. The set up also contains a *KineOptics* WTB 2.0 axis force cell balance, and two 250 g *Honeywell* Model 11 load cells with an accuracy of 0.14 mV/V. The *National Instruments* data acquisition system included a NI-9237 bridge module which has an accuracy of 0.2% of reading and a resolution of 1.2 mV, a NI-cDAQ 9178 CompactDAQ chassis, two RJ-50 cables, three 6' BNC cables, and a BNC-to-Banana plug adapter. A PC equipped with *LabView* software called 'windtunnel main.vi' program was used to operate the system. Before the experiment began, the load cells were zeroed using the 'Null' command. In addition to the wind tunnel setup, a testing model and *McMaster*: 1787T12 calibration weights were used to collect the data needed for the lift load cell calibration curve. For the drag load cell calibration a *Correx* 500cN force meter with round probe end from *Long Island Indicator Service* was used and has an accuracy of 0.01\*500cN, and a resolution of 5 cN. Figure 1 below shows the general lab setup.

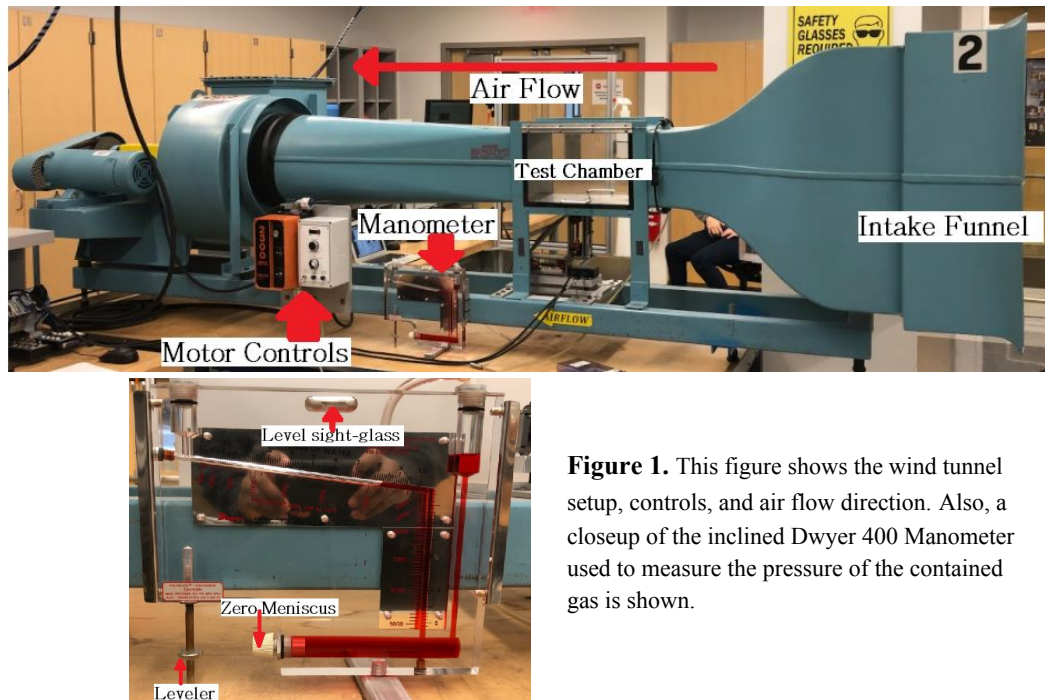


**Figure 1.** This figure shows the wind tunnel setup, controls, and air flow direction. Also, a closeup of the inclined Dwyer 400 Manometer used to measure the pressure of the contained gas is shown.

## Model Truck Measurements

In order to perform calculations involving the drag and lift coefficients, each model truck was measured in order to determine their characteristic length,  $L$ , planform area,  $A_L$ , and frontal area,  $A_D$ . Each truck was measured using a Matsuyo digital caliper with a resolution error of  $\pm 0.01$  mm and accuracy error of  $\pm 0.02$  mm. The characteristic length was defined to be the length of the truck from front to back,  $L$ . In order to determine planform area,  $A_L$ , and frontal area,  $A_D$ , the width,  $w$ , and height,  $h$ , were measured. Planform area,  $A_L$ , and frontal area,  $A_D$ , are defined by Equations 1 and 2 [4] below.

$$A_L = L * w \quad (\text{Eqn 1})$$

$$A_D = h * w \quad (\text{Eqn 2})$$

Figure 2 below shows where each measurement is taken from a sample truck.

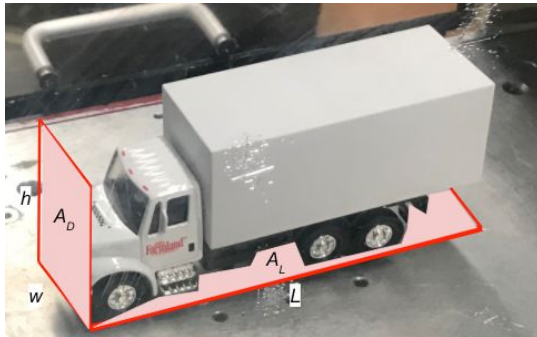


**Figure 2.** This figure shows where the measurements for width,  $w$ , height,  $h$  and length,  $L$ , are taken on the truck. It also shows how the planform area,  $A_L$ , and frontal area,  $A_D$ , are defined.

## Lift & Load Cell Calibration

In order to calibrate the load cell for lift, the test model was installed on the threaded spindle using an allen wrench and aligned corresponding to air flow and the load cells were zeroed again. Then, an ASTM class 7 calibration weight was placed on top of the test model and the ‘Take Data’ command was selected in *LabView*. After the test was completed the mass of the calibration weight and lift reading reported on *LabView* were both recorded, with error. The calibration weight was removed and the previous steps were repeated for a series of six masses, ranging from 10g to 200g. After all values were collected a plot of the applied vertical force and the output load cell voltage was generated with the lift correlation factor expressed as the slope of the line of best fit. Figure 3 below shows the setup for the lift load cell calibration.

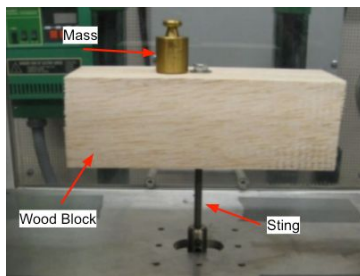


**Figure 3.** This image shows an example of the setup of the lift load cell calibration.

## Drag Load Cell Calibration

The drag load cell calibration model is similar to the lift load cell. First, the load cells were zeroed and the force meter was used to apply a lateral force-load to the block. The feeler arm of the force meter was always positioned at right angles to the direction of the force. Next, the ‘Take Data’ command was selected on *LabView* and the applied lateral force and drag reading reported on *LabView* were recorded. The lateral force was removed and the previous steps were repeated for a series of different forces in both directions, ranging from -200 to 200 cN. After all values were collected a plot of the applied lateral force

and the output load cell voltage was generated, with the drag correlation factor expressed as the slope. Figure 4, on the following page, shows the setup of the drag load cell calibration.

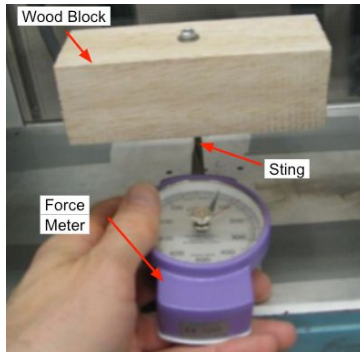


**Figure 4.** This image shows a sample test setup for the drag load cell, with the force applicator shown in hand.

### Wind Tunnel Testing

After the dimensions of each truck were taken, and the load cells were calibrated, the magnetic overload rod was verified to be properly aligned in the wind tunnel, the manometer was leveled using the threaded leveling foot at its base, the manometer incline was zeroed using the white knob near the base to adjust the position of the meniscus, and the controller was set to 'Local' mode. The temperature and air pressure of the testing room was recorded from the TE388W *Meade Instruments* weather station which had a resolution of 0.2 °F and a pressure resolution of 0.02 in-Hg. A test model was installed on the threaded spindle aligned accordingly with the air flow. The load cells were zeroed and the wind tunnel controller was turned on while the controller switch was moved to the 'Run' position. The motor speed knob was adjusted until the manometer reading was the same as that of the manometer readings from the wind speed calibration, so the recorded wind speed was more accurate than the digital reading. The 'Take Data' command was then selected on *LabView*. Once the test was completed a data file containing the time, lift, and drag data from the test was saved. At the end of the experiment the switch was moved to the 'Stop' position and the wind tunnel controller was turned off. This operation was then completed for the remaining test models at each desired speed. This test was also done with just the sting, so that we could know what portion of the drag and lift come from the sting. The four model trucks are shown below in Figure 5, along with a sample truck placed in the test area. The last model tested was a truck without a container attached.

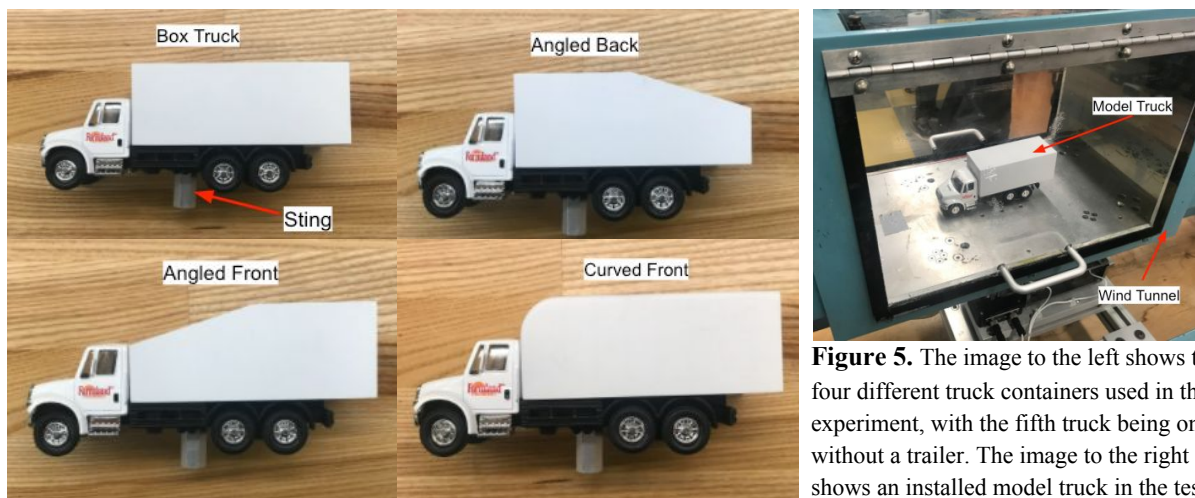


**Figure 5.** The image to the left shows the four different truck containers used in this experiment, with the fifth truck being one without a trailer. The image to the right shows an installed model truck in the test chamber.

## Force Conversion

After data from the wind tunnel tests was collected, the drag and lift readings in mV/V needed to be converted to a force. To do this, we used the calibration curves for the drag and lift load cell. The drag correlation equation, which was determined to be the equation of the line of best fit for the drag calibration data, was applied to the drag voltage reading of each test. This gave the drag force acting on each truck at each wind speed in SI units. This process was repeated using the lift correlation equation and the lift voltages in order to determine the lift forces acting on each truck for each wind speed. These calculated lift and drag forces were then plotted versus the calculated wind speed for each truck, with error calculated using the root sum square method. The lift and drag forces of the sting were subtracted from the truck lift and drag data to mitigate the effect of this additional piece on the data.

## Manometer Reading

To calculate the flow velocity, the density of the air in the lab is needed. The density of air in our lab conditions,  $\rho$ , was calculated using Equation 3, where  $P_B$  is the absolute pressure of the room in in-Hg, and  $T$  is the temperature of the room in degrees Celsius. The flow velocity can then be calculated using a simplified form of Bernoulli's principle, Equation 4, where  $v$  is the air flow velocity in m/s, and  $P_v$  is the pressure measured by the manometer (atmospheric pressure - chamber pressure) in units of in-H<sub>2</sub>O, and  $\rho$  is density in units of kg·m<sup>-3</sup>.

$$\rho = 0.8867 \cdot \frac{P_B}{T} \quad (\text{Eqn 3})$$

$$v = 22.309 \cdot \sqrt{\frac{P_v}{\rho}} \quad (\text{Eqn 4})$$

## Dimensionless Parameters

The dimensionless parameters, lift and drag coefficients, were calculated using Equations 5 and 6 [3]. In those equations,  $v$  is the air flow velocity reported by manometer reading,  $A_L$  is the planform area,  $A_D$  is the frontal area,  $F_L$  is the lift force, and  $F_D$  is the drag force. The Reynolds number was calculated using Equation 7 [4], where  $\rho$  is the density of air,  $v$  is the air stream velocity, and  $\mu$  is the dynamic viscosity of air, and  $L$  is the model's characteristic length.

$$C_L = \frac{2F_L}{\rho v^2 A_L} \quad (\text{Eqn 5})$$

$$C_D = \frac{2F_D}{\rho v^2 A_D} \quad (\text{Eqn 6})$$

$$Re = \frac{\rho v L}{\mu} \quad (\text{Eqn 7})$$

## Forces Acting on Full-Scale Truck

In order to calculate the forces acting on the full-scale truck, the dimensionless parameters need to be related between the model (1:55 model truck) and prototype (full-scale truck). The dimensionless parameters considered are the Reynolds number and the lift and drag coefficients. To accurately compute the forces acting on the full-scale truck, the Reynolds number of the model and prototype must be matched in the wind tunnel test. Then by using the lift and drag coefficients that are computed for the model as a result of the test, the lift and drag forces acting on the prototype can be calculated via a manipulation of Equation 5 and 6 and substituting in values for  $v$  and  $A_L/A_D$  which correspond to the prototype.

Due to the scale of the model being so small (1:55), the required velocity in the wind tunnel in order to match Reynolds numbers would be 55x that of the wind speed experienced by the prototype, which is deep into the supersonic range of wind speeds. Due to our testing limitations, we are unable to achieve the

matching of Reynolds numbers, either through these higher wind speeds or by manipulation of the working fluid. We will account for this limitation by extrapolating our lift and drag coefficients as the average of the coefficients we calculated in the range of Reynolds numbers which were tested. The forces experienced by the full-scale truck are then calculated using Equations 8 and 9, where the average value is represented by a bar over the variable and prototype (full-scale truck) values are denoted with a subscript  $p$ .

$$F_{L,p} = \frac{1}{2} \cdot \overline{C_L} \cdot \rho \cdot v_p^2 \cdot A_{L,p} \quad (\text{Eqn 8})$$

$$F_{D,p} = \frac{1}{2} \cdot \overline{C_D} \cdot \rho \cdot v_p^2 \cdot A_{D,p} \quad (\text{Eqn 9})$$

## RESULTS

This section presents the analysis of the wind tunnel tests in order to determine: the calibration curves of the load cell and manometer; the lift and drag forces as a function of calibrated wind speed for all provided truck models; the lift and drag coefficients as a function of Reynolds number for each of the provided truck models; the truck/container combination that results in the lowest average drag coefficient within the measurement range of Reynolds number; and our prediction of the lift and drag forces on a full-scale truck at a moving speed of 65 miles per hour, using the truck/container combination with the lowest average drag coefficient. Uncertainty is propagated from measured quantities where applicable via root mean square method and the partial derivative formula [5].

### Load Cell Calibration

The drag and lift force load cell calibration curves from data gathered during calibration are shown below in Figure 6. These calibrations are used to determine the drag and lift forces acting on each model truck at each wind speed by using the line of best fit. The figures below give the drag and lift force in cN as a function load cell readout in mV/V. These calculated functions from the calibration curves are used in each wind tunnel test to convert from load cell output, [mV/V], to a force output, [cN], with error.

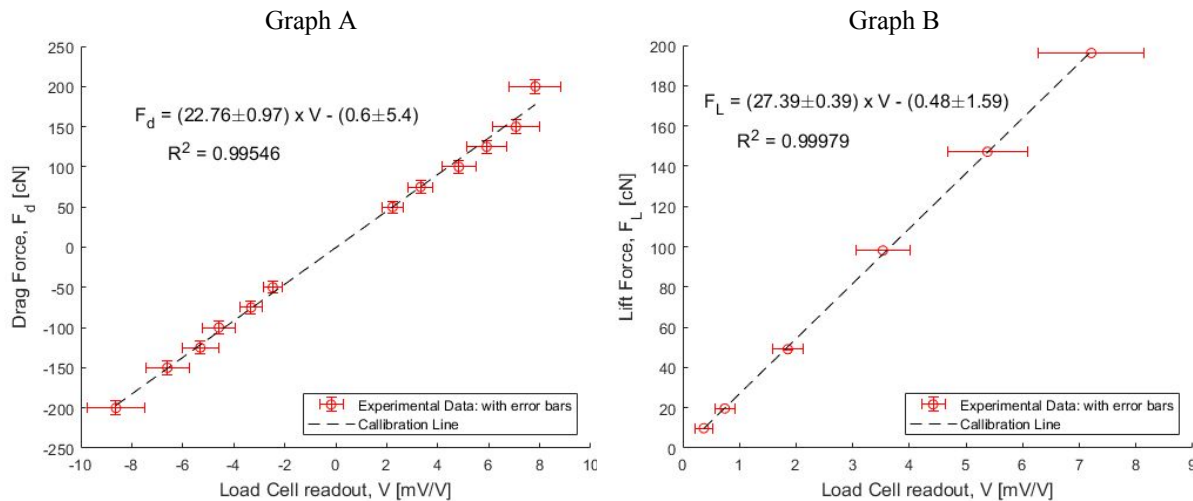


**Figure 6.** This figure shows the calibration curves for drag force, Graph A, and lift force, Graph B, versus the voltage readout of the *Honeywell* Subminiature load cell. Graph A has a maximum load cell error of  $\pm 1.1$  [mV/V] and a maximum drag force error of  $\pm 8.6$  [cN]. The drag force calibration slope is  $22.76 \pm 0.97$  [cN/(mV/V)] with an intercept of  $-0.6 \pm 5.4$  [cN]. Graph B has a maximum load cell error of  $\pm 0.93$  [mV/V] and maximum lift force error of  $\pm 0.18$  [cN]. The lift force calibration slope is  $27.39 \pm 0.39$  [cN/(mV/V)] with an intercept of  $-0.48 \pm 1.59$  [cN].

### Wind Velocity Calibration

In order to determine the exact wind speed that the model was subject to, a wind speed calibration is given below in Figure 7. This figure shows the relationship between the nominal wind speed reading on

the wind tunnel, and the actual wind speed calculated using Equations 3 and 4. Equation 3 was used to calculate the density of the air in the laboratory, which was found to be  $1.225 \pm 0.03 \text{ kg}\cdot\text{m}^{-3}$ . This value for air density was then plugged into Equation 4, along with the manometer pressure readings, which was used to calculate the actual wind speed. During testing, we set the wind speed by setting the manometer reading rather than setting the nominal wind speed on the wind tunnel, so this calibration curve is not used in our further analysis. Rather, the calculated wind speeds based on our manometer readings are used for each calculation.

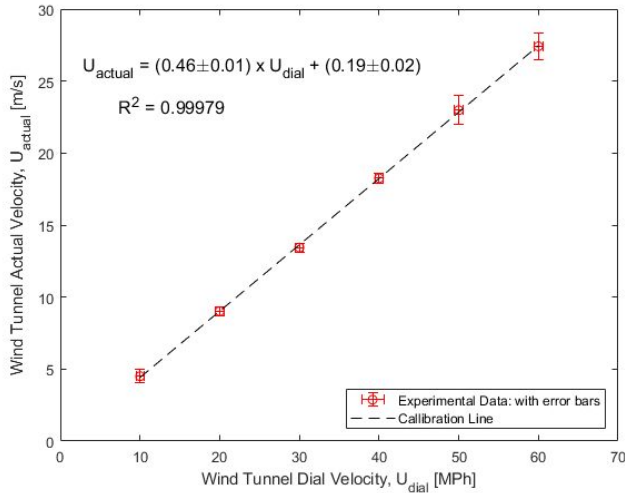


**Figure 7.** This figure shows the calibration curve for converting the wind tunnel dial readout into air velocity in the wind tunnel. The maximum error on the dial readout is  $\pm 0.52$  [mph] and the maximum error on the true wind velocity is  $\pm 1.0$  [m/s]. The increased error seen on the last two points for actual velocity was caused by the lower resolution of the manometer for readings greater than 1 [in-H<sub>2</sub>O]. The dial velocity readout calibration slope is  $0.46 \pm 0.01$  [(m/s)/mph] with an intercept of  $0.19 \pm 0.02$  [m/s].

## Force Plots

After converting the load cell voltage readouts to forces using the load cell calibration curves above, we were able to plot the drag force and lift force acting on each model truck at each wind speed, which were calculated according to the procedure discussed in the Methods section. Figure 8 below shows each graph of drag force and lift force versus wind speed for each of the five model trucks.

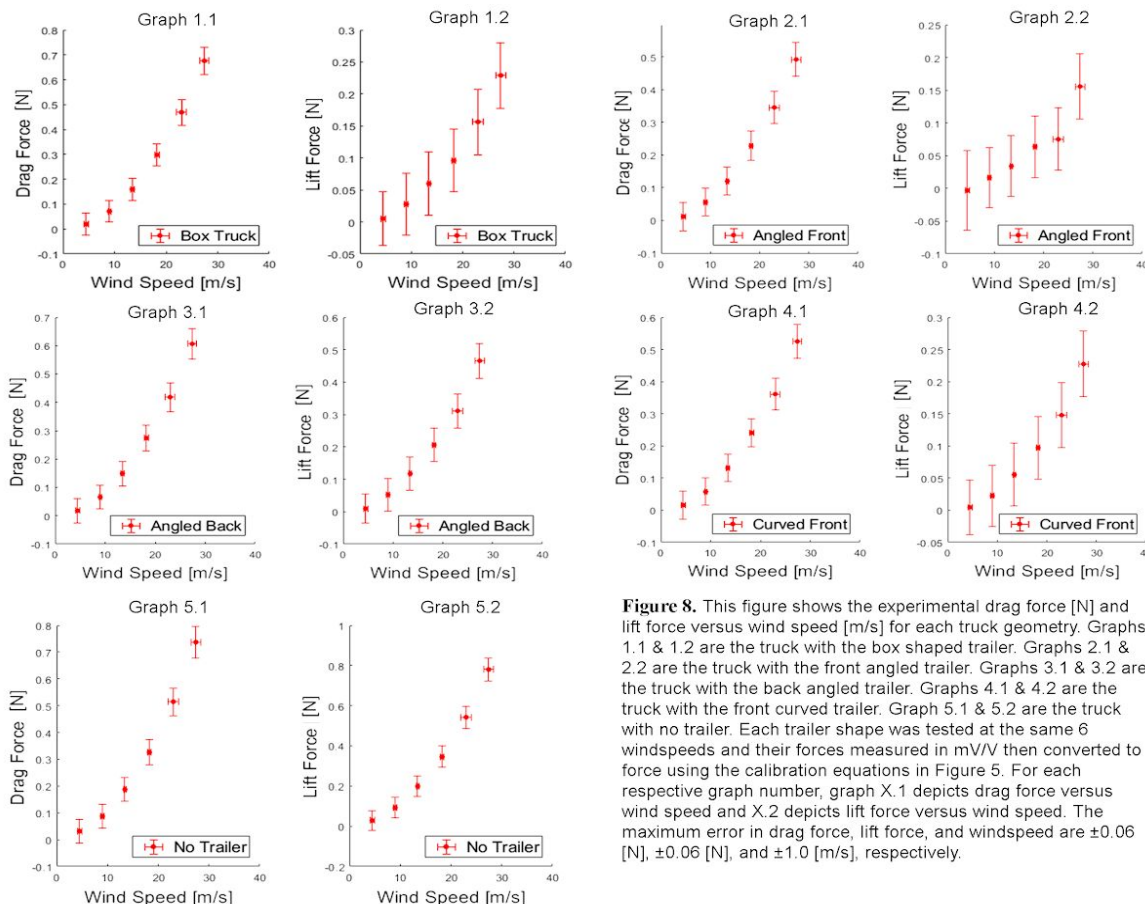


**Figure 8.** This figure shows the experimental drag force [N] and lift force versus wind speed [m/s] for each truck geometry. Graphs 1.1 & 1.2 are the truck with the box shaped trailer. Graphs 2.1 & 2.2 are the truck with the front angled trailer. Graphs 3.1 & 3.2 are the truck with the back angled trailer. Graphs 4.1 & 4.2 are the truck with the front curved trailer. Graph 5.1 & 5.2 are the truck with no trailer. Each trailer shape was tested at the same 6 windspeeds and their forces measured in mV/V then converted to force using the calibration equations in Figure 5. For each respective graph number, graph X.1 depicts drag force versus wind speed and X.2 depicts lift force versus wind speed. The maximum error in drag force, lift force, and windspeed are  $\pm 0.06$  [N],  $\pm 0.06$  [N], and  $\pm 1.0$  [m/s], respectively.

## Drag and Lift Coefficient Calculations

Using the drag and lift force data from the wind tunnel tests, the drag and lift coefficients were calculated for each of the five truck models using Equations 5 and 6 above, along with error. The Reynolds number for each model truck at each wind speed was calculated using Equation 7, along with error, where  $\mu$ , dynamic viscosity, was determined to be  $(1.8258 \pm 0.02) \times 10^{-5} \text{ kg/m}\cdot\text{s}$  [3], with error calculated using the direct sampling method. Reynolds number versus drag coefficient and Reynolds number versus lift coefficient for each truck is plotted below in Figure 9.

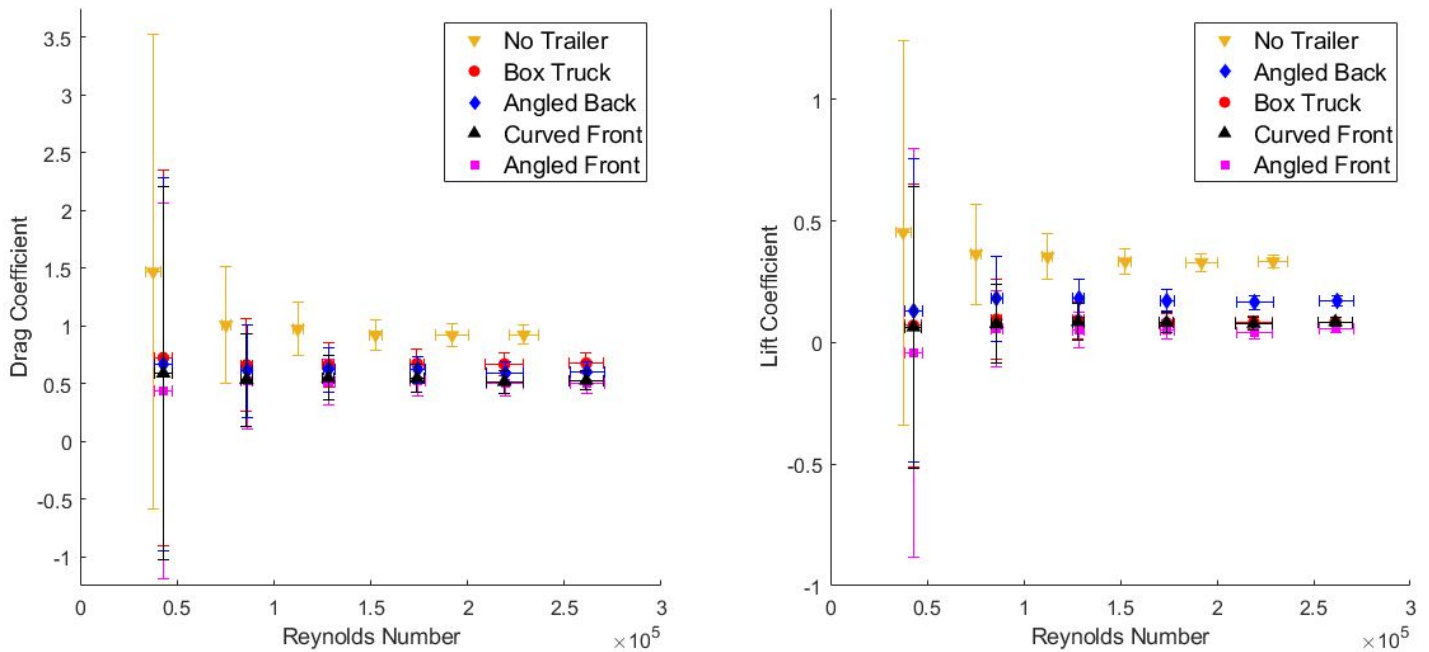


**Figure 9.** This figure shows a graph of Reynolds number versus drag coefficient and lift coefficient for each model truck. The large error bars on the first few points are due to the magnitude of the accuracy error of the Honeywell Subminiature Load Cell, which is 0.14 mV/V. This error is nearly twice the initial voltage readings for lift and drag at low wind speeds, which makes the accuracy error more than the reading, explaining the large error. The maximum drag coefficient, lift coefficient, and Reynolds number error were  $\pm 2.1$ ,  $\pm 0.79$ , and  $\pm 9.6 \times 10^3$  respectively.

In order to more easily show the relative calculated drag and lift coefficients between the different models, Figure 10 on the page below shows the same data as Figure 9 above but without error bars and zoomed in axes. This allows the model truck with the lowest drag coefficient, the Angled Front container, to be picked out more easily.

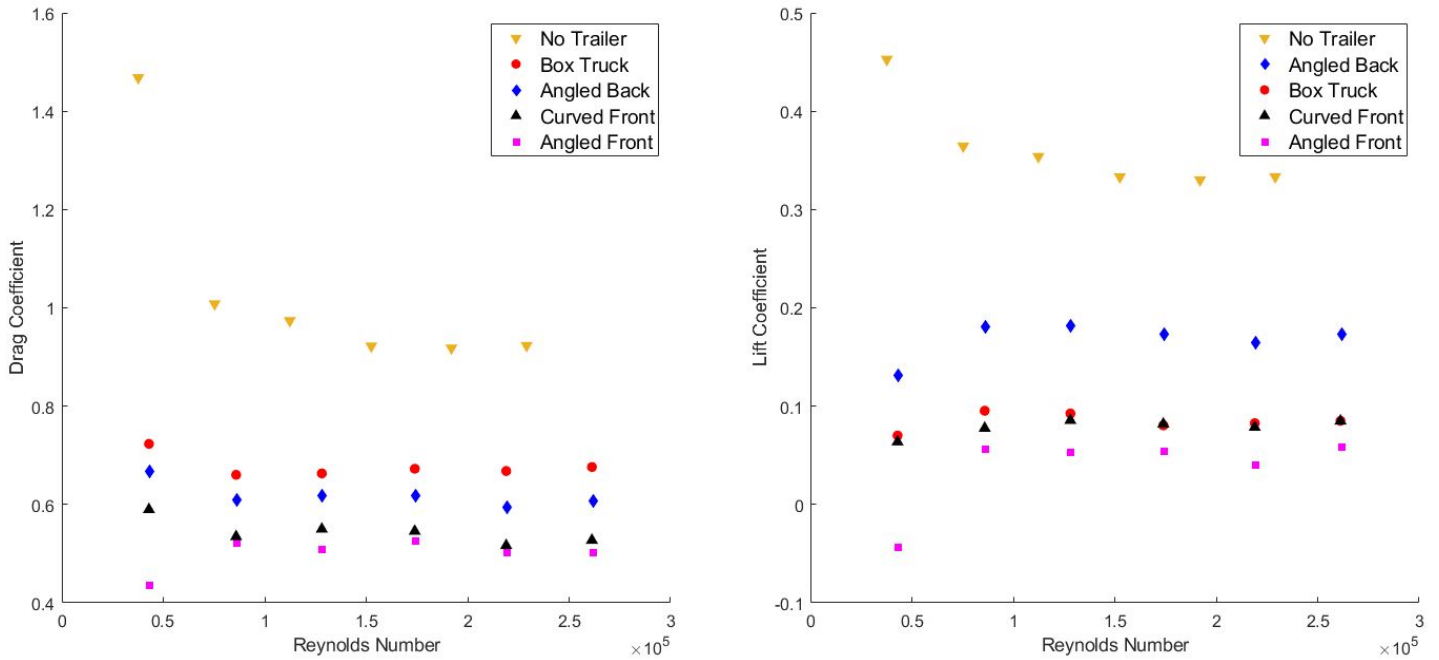


**Figure 10.** This figure shows the calculated drag and lift coefficients for each truck without error bars. This allows the values to be compared relative to each other more easily. By visual assessment, the Angled Front truck/container has the lowest average drag coefficient over the range of Reynolds numbers we tested.

The average values of drag coefficient and lift coefficient were then calculated for each truck over the entire range of Reynolds numbers we tested. The averaged values for each coefficient for each truck is given below in Table 2.

**Table 2.** This table shows the calculated average drag and lift coefficients for each truck trailer combination, along with error.

Truck Assembly	Avg. Drag Coefficient	Avg. Lift Coefficient
Box Truck	0.68±0.42	0.08±0.15
Angled Front	0.50±0.43	0.03±0.09
Angled Back	0.62±0.42	0.17±0.16
Curved Front	0.54±0.42	0.08±0.15
No Trailer	1.04±0.67	0.36±0.21

### Full-Scale Force

As shown above in Table 2, the container design with the lowest average drag coefficient was the angled-front container. This truck/container combination's average coefficient of drag and lift were then used to calculate the drag and lift forces that would occur on a full-scale truck of the same shape at a moving speed of 65 miles per hour. This calculation assumes that the absolute wind speed is zero (still ambient air) and therefore the wind speed used in the calculation is 65 miles per hour, or 29.06 m/s. Using a planform lift area,  $A_{L,p}$ , and frontal drag area,  $A_{D,p}$ , which are  $55^2$  times larger than the corresponding model's (model is 1:55 scale for each dimension), the forces due to lift and drag are calculated using Equations 8 and 9.

The resulting lift force acting on the full-scale truck was calculated to be around  $330 \pm 8.8 \times 10^2$  N (opposing gravitational pull) and the drag force was calculated to be around  $1700 \pm 1.4 \times 10^3$  N (opposing the direction of travel of the truck). As mentioned earlier, the Reynolds numbers were not able to be matched 1:1 for model and prototype, and therefore there are validity issues arising, introducing uncertainty in this estimation. As studies have shown, the transition from laminar flow to turbulent flow brings about a reduction in the drag coefficient, marked by a critical Reynolds number [2]. For our tests, the model's Reynolds number maximized in the range of lower  $10^5$  values (approx.  $2.6 \cdot 10^5$ ), while the

calculated Reynolds number for the full-scale truck moving at 65 mph had a value of low  $10^7$  (approx.  $1.5 \cdot 10^7$ ). Upon researching the effects of the turbulent flow transition on drag coefficients, Figure 11 shows the relationship between drag coefficient and Reynolds number for two different geometries, emphasizing the critical Reynolds numbers [2].

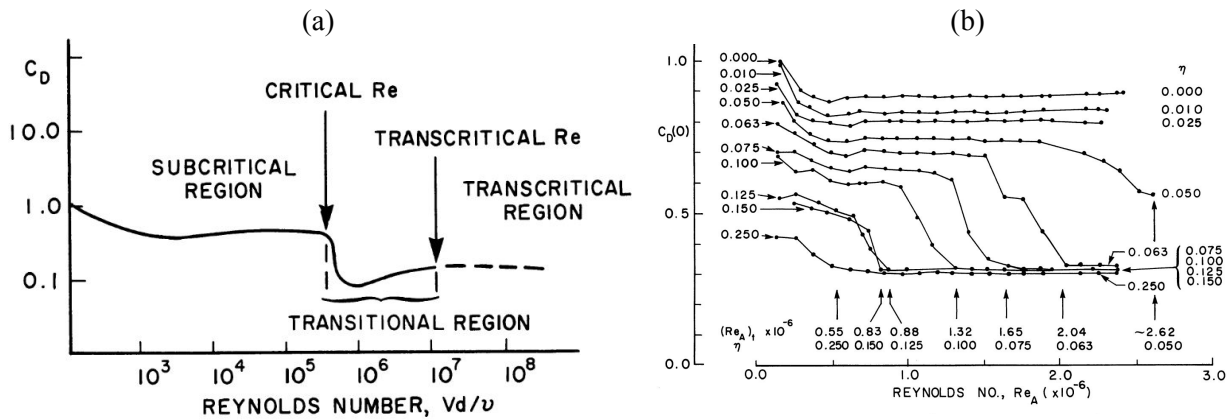


**Figure 11.** Graph (a) shows the relationship between the drag coefficient and Reynolds number for flow around a sphere, with a notable critical Reynolds number of somewhere between higher  $10^5$  and lower  $10^6$  for the transition between laminar and turbulent flow. Graph (b) shows the findings of Kevin R. Cooper’s paper on the relation between drag coefficient and Reynolds number for bluff bodies as a function of front-edge rounding,  $\eta$ . These results corroborate the critical Reynolds number being in the range of  $10^5$  and  $10^6$  (for bluff bodies rather than a sphere), with certain geometries reaching into the lower  $10^6$  range for critical Reynolds numbers.

From these observations, it is apparent that due to our testing range of Reynolds numbers being lower than the critical Reynolds number (somewhere in the range of large  $10^5$  or low  $10^6$ ), we may overestimate the forces acting on the full-scale truck due to the model not being tested under turbulent flow conditions. As seen in Figure 11 (a) and (b), above, the drag coefficient decreases after the critical Reynolds number and settles in the transcritical region to a value which is lower than the subcritical region. Since the forces acting upon the body are linear with respect to the lift and drag coefficients, we expect a similar decrease in the force upon entering the transitional and transcritical regions. We expect this to be the case for the full-scale truck, given your trucks’ operating cruise conditions.

## CONCLUSIONS

Based on the procedures and results described above, we recommend using a container with a flat chamfer on the front end as depicted in the image labeled “Angled Front” in Figure 5 in the Methods section. At speeds that result in a Reynolds numbers below the critical value, characterized as laminar flow, this trailer shape resulted in the lowest average drag and lift coefficients of the trailer shapes tested with an average drag coefficient of  $0.5 \pm 0.43$  and an average lift coefficient of  $0.03 \pm 0.09$  at 1:55 scale. These drag and lift coefficients correspond to an estimated drag force of  $1700 \pm 1.4 \times 10^3$  N and a lift force of  $330 \pm 8.8 \times 10^2$  N when the experiment results are applied to a 1:1 full scale truck driving 65 mph. The force and coefficient estimates for all full scale trailer truck combinations are listed in Table 3 on the following page.

**Table 3.** This table shows the estimated Reynolds number, and drag and lift coefficients and forces for the full scale truck based on the data collected on the 1:55 scale models provided.

Trailer Shape	Avg. Drag Coefficient	Drag Force [N]	Avg. Lift Coefficient	Lift Force [N]	Estimated Reynolds Number
Box	0.68±0.42	2300.8±1.4x10 <sup>3</sup>	0.08±0.15	286.5±5.2x10 <sup>2</sup>	1.4x10 <sup>7</sup> ±5.2x10 <sup>5</sup>
Angle Front	0.50±0.43	1695.0±1.5x10 <sup>3</sup>	0.03±0.09	122.6±3.3x10 <sup>2</sup>	1.4x10 <sup>7</sup> ±5.2x10 <sup>5</sup>
Angle Back	0.62±0.42	2103.6±1.4x10 <sup>3</sup>	0.17±0.16	568.9±5.5x10 <sup>2</sup>	1.4x10 <sup>7</sup> ±5.2x10 <sup>5</sup>
Curved Front	0.54±0.42	1847.7±1.4x10 <sup>3</sup>	0.08±0.15	267.3±5.1x10 <sup>2</sup>	1.4x10 <sup>7</sup> ±5.2x10 <sup>5</sup>

We would like to qualify the previous recommendation with an acknowledgement that there are three significant factors to keep in mind when reading this result:

- First, all of the coefficient errors of tested trailer shapes leave the average drag and lift coefficients well within the error regions of the front angled trailer, as seen in Table 3. This is in large part due to the accuracy error of the load cell used to measure the drag and lift forces on each test of 0.14 [mV/V]. This could be mitigated by conducting future testing with more accurate equipment.
- Second, though trailer volumes were not explicitly evaluated, it appears likely that the sample geometries provided do not all possess the same volume and therefore would not be able to transport the same volume of goods. This would make direct comparison of drag coefficient an inadequate metric for determining which geometry best suits your company's needs. In order to adequately recommend a geometry we would need to know: the marginal utility of trailer volume changes relative to cargo value, the average efficiency of the engines in your trucks relative to the mass of the load they carry, your average cost of fuel, the volume of fuel your trucks can carry, and the average density of the fuel used. This would allow us to better evaluate the marginal utility of increases in container volume to marginal costs of increases in drag forces and relate both to overall fuel efficiency.
- Third, given that the Reynolds numbers of the scale models stayed primarily under the critical value differentiating laminar and turbulent flows, the drag and lift coefficients produced likely will not reflect the true drag and lift coefficients for the full scale geometries. In order to account for this, we recommend testing with a model larger than one with a 1:55 scale, as well as increasing testing speeds to ensure that the Reynolds number of future testing conditions reaches well past the critical value ( $Re \sim 10^6$ ) in order to better estimate drag coefficients in turbulent conditions.

In conclusion, we can hypothesize that, of the four container geometries tested, a front angled cargo container will produce the lowest drag coefficient, which would optimize the efficiency of your fleet, assuming no losses in cargo capacity. The tests conducted are not fully conclusive and we recommend further testing so that the scale model results are more representative of full scale performance and better simulate the turbulent flows your trucks will experience when traveling at 65 mph.

## REFERENCES

- [1] Aerolab. (2014). *Educational Wind tunnel*. Aerolab LLC. PDF file.  
<https://mdn0r3kvarr35bepm3komzo4-wpengine.netdna-ssl.com/wp-content/uploads/2014/08/AEROLAB-EWT-Brochure-4.pdf>
- [2] Cooper, David R. *The Effect of Front-Edge Rounding and Rear-Edge Shaping on the Aerodynamic Drag of Bluff Vehicles in Ground Proximity*. SAE Transactions, Vol. 94, Section 2 (1985), pp. 727-757
- [3] Engineering ToolBox, (2003). *Air - Dynamic and Kinematic Viscosity*. [online] Available at: [https://www.engineeringtoolbox.com/air-absolute-kinematic-viscosity-d\\_601.html](https://www.engineeringtoolbox.com/air-absolute-kinematic-viscosity-d_601.html) [Accessed 07 Dec. 2020].
- [4] Gerhart P, Gerhart A, Hochstein, Munson, Okiishi, and Young, *Fundamentals of Fluid Mechanics*. Hoboken, NJ: John Wiley & Sons, Inc.; 2016.
- [5] Taylor, J.R. (1997), *An Introduction to Error Analysis*, 2nd ed., University Science Books, Sausalito, California.